Four-wave mixing resonantly enhanced by ac-Stark-split levels in self-trapped filaments of light

Donald J. Harter* and Robert W. Boyd
Institute of Optics, University of Rochester, Rochester, New York 14627
(Received 24 June 1983)

It is observed that when an intense, nearly resonant laser beam propagates through a dilute ($N < 5\times 10^{14}$ cm^{-3}) vapor of sodium atoms, a four-wave-mixing process occurs, leading to the generation of strong, coherent radiation in the forward direction at frequencies symmetrically detuned from that of the exciting laser by the generalized Rabi frequency. This phenomenon is explained as resulting from a nearly phase-matched mixing process utilizing the nonlinear response of the sodium atom. Our analysis is based on a solution of the density-matrix equations of motion that includes the effect of level shifts induced by the ac Stark effect, which can be as great as 10 Å for our experimental conditions, and which leads to gain due to the stimulated three-photon effect at one Rabi sideband and to strong coupling due to a parametric mixing process between radiation at the two sideband frequencies. It is also observed that at larger sodium densities ($N \gtrsim 5\times 10^{14}$ cm^{-3}), self-focusing of the laser beam can occur, leading to several complicating effects. We find experimentally that the on-resonance Rabi frequency Ω within a self-trapped filament lies preferentially within the range from 1 to 3 times the laser detuning from resonance Δ and we explain this result as a consequence of strong saturation of the refractive index that occurs for $\Omega \gtrsim \Delta$. Four-wave mixing is found to occur within these self-trapped filaments. The high-frequency sideband thus generated is trapped within the filament, whereas the lower-frequency sideband is ejected as a consequence of Snell's law and forms a cone surrounding the transmitted laser beam.

I. INTRODUCTION

An intense, near-resonant laser field can profoundly modify the absorption and emission spectra of an atomic system. This modification can be understood conceptually as resulting from the shifting and splitting of atomic energy levels due to the ac Stark effect[1] or equivalently to the "dressing" of the atom due to its interaction with the laser field leading to pairs of dressed levels separated by the generalized Rabi flopping frequency.[2] Such effects were first studied at microwave frequencies by Autler and Townes[3] and only more recently have been studied at optical frequencies where propagation effects and the possibility of spontaneous emission introduce new aspects to the problem. At optical frequencies these effects were first studied in spontaneous emission, for which case it was predicted by Mollow[4] and confirmed experimentally by Schuda *et al.*[5] that for large laser intensities resonance fluorescence has a three-peaked spectrum with adjacent components separated by the Rabi frequency.

The resonances of stimulated processes are similarly modified. Wu *et al.*[6] have observed gain at one Rabi sideband and absorption at the other for the case of an intense, near-resonant laser beam interacting with the sodium atom. Using theoretical methods introduced by others,[7–9] Harter and Boyd[10] have shown the existence of a strong resonance in the four-wave mixing $\chi^{(3)}$ susceptibility for weak fields detuned symmetrically by the generalized Rabi frequency from the frequency of an intense pump field. It was further shown by Boyd *et al.*[11] that for the case of nearly copropagating beams, this strong coupling between the Rabi sidebands can lead to gain for both sidebands. The generation of intense radiation at both sideband frequencies has been observed by Harter *et al.*[12] and subsequently by Kleiber *et al.*[13] and Burdge and Li.[14] In these experiments using pulsed dye lasers, extremely large values of the Rabi frequency are attainable, leading to ac Stark shifts of the atomic energy levels by as much as 10 Å. In the work of Harter *et al.*[12] it was noted that under many experimental conditions self-focusing occurs simultaneously with Rabi sideband generation and that the spatial and temporal structure of the emitted radiation is greatly modified by the self-focusing process. In the present paper we present a detailed account of our experimental results with particular emphasis placed on the self-focusing process and its influence on the four-wave-mixing process leading to Rabi sideband generation. We have found that, under rather broad circumstances, self-focusing can lead to the generation of stable self-trapped filaments of light and that four-wave mixing occurring within such filaments can lead to the emission of red-shifted radiation in the form of a cone surrounding the laser beam. We believe that the cone of light observed by Skinner and Kleiber[15] and by Tam[16] is likely to result from processes similar to those discussed here.

II. FOUR-WAVE MIXING

The efficiency of a four-wave-mixing process is greatly enhanced when the interacting waves are close in frequency to an atomic resonance. The resonances of the four-wave-mixing process can be shifted as a result of ac Stark

effects, as shown in Fig. 1. A strong pump laser of field amplitude E_1 and frequency ω_1 is detuned to the high-frequency side of an atomic resonance by an amount $\Delta=\omega_1-\omega_{ba}$, where ω_{ba} denotes the unperturbed atomic-resonance frequency. The effect of the strong applied laser is to split both the upper and lower atomic levels into pairs of "dressed states" separated by the generalized Rabi frequency

$$\Omega'=(\Omega^2+\Delta^2)^{1/2}, \tag{1}$$

where $\Omega=\mu_{ba}E_1/\hbar$, with μ_{ba} denoting the dipole matrix element for the transition between the atomic levels, and Ω denoting the Rabi frequency. As a result, the parametric mixing process shown on the right side of Fig. 1 is strongly resonantly enhanced at each of the intermediate levels. Spontaneous emission from the ac-Stark-shifted energy levels (or any broadband background radiation) can be amplified by this four-wave-mixing process, leading to the generation of intense radiation at frequencies $\omega_1\pm\Omega'$. These new frequency components can be considered to be Rabi sidebands impressed upon the transmitted laser beam by the Rabi flopping of the strongly driven atomic system. As drawn in Fig. 1, Δ is positive as it is in most of our experimental work. For this sign of the detuning, in the steady state the upper component of the lower pair is more highly populated than the lower component. The three-photon wave at frequency $\omega_3=\omega_1+\Omega'$ can then experience gain by the stimulated three-photon effect,[17] while the fourth-parametric wave at $\omega_4=\omega_1-\Omega'=2\omega_1-\omega_3$ can experience gain *only* by means of the parametric interaction illustrated in this figure.[11] For the opposite case of a negative detuning, three-photon gain occurs at $\omega_1-\Omega'$, while parametric processes can amplify a wave at $\omega_1+\Omega'$.

The gain experienced by a weak probe wave interacting with a collection of atoms is shown for a representative case in Fig. 2. This curve is a plot of Eq. (25) of Ref. 11 which was derived by solving the coupled amplitude equations of nonlinear optics with a nonlinear susceptibility obtained from the solution of the density-matrix equations of motion for a two-level atom. Phenomenological decay times T_1 and T_2 were incorporated into this model and

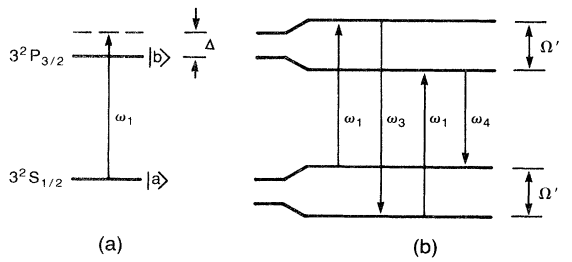

FIG. 1. (a) Intense optical field of frequency ω_1 is detuned by an amount Δ from the $3^2S_{1/2}$-$3^2P_{3/2}$ (D_2) resonance transition of sodium. (b) As a result of the ac Stark effect the upper and lower levels are split into doublets separated by the generalized Rabi frequency Ω'; leading to a strong resonance enhancement of the illustrated four-wave-mixing process.

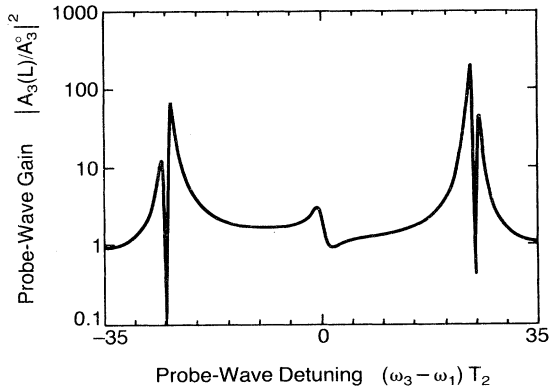

FIG. 2. Gain experienced by a probe wave interacting with a collection of strongly driven two-level atoms is shown as a function of the detuning of the probe wave from the pump wave. This curve is obtained by solving the coupled wave equations with a nonlinear susceptibility given by the steady-state solution of the density-matrix equations of motion, as described in Ref. 11. Strong resonances are observed near the Rabi sidebands. The calculation assumed the following parameters: $(\omega_1-\omega_{ba})T_2=8$, $\Omega T_2=25$, $T_2/T_1=0.02$, $\Delta k=0$ (i.e., perfect phase matching) and $\alpha_0 L=2500$, where α_0 denotes the weak-field line center absorption coefficient.

solutions were found that are correct to all orders in the amplitude of the strong field at ω_1 and are also correct to lowest order in the amplitudes of the waves at ω_3 and ω_4. The curve shows strong enhancement of the gain in the vicinity of the Rabi sideband frequencies, in agreement with the intuitive picture presented in Fig. 1. The sharp dip that occurs exactly at the Rabi sideband frequency results from our assumption of perfect phase matching. It is shown in Ref. 11 that if Δk is allowed to take on nonzero values, broad structureless resonances centered at the Rabi sideband frequencies are predicted. Figure 3 illustrates how the gain at the Rabi sideband frequencies depends on

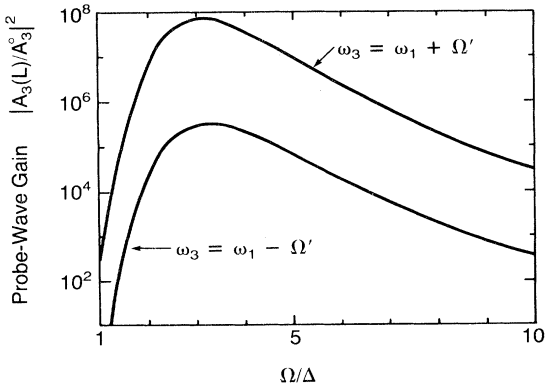

FIG. 3. Probe-wave gain at the Rabi sidebands (i.e., $\omega_3-\omega_1\pm\Omega'$) is shown as a function of Ω/Δ with Ω' fixed at a value of $15/T_2$. The curve was calculated as described in Fig. 2 and assumed the parameters $T_2/T_1=2$ and $\alpha_0 L=100$, with Δk selected numerically to maximize the probe-wave gain. The curves show substantial gain for Ω/Δ in the observed range of approximately 1 to 3.

the ratio Ω/Δ for a representative case. It is seen that significant gain occurs for Ω/Δ in the range 1—4 which, as is discussed later, is approximately the range of values where significant Rabi sideband generation is observed experimentally.

Previously, Harter *et al.*[12] have reported the generation of intense radiation at the Rabi sideband frequencies in the forward direction in sodium vapor (in the absence of laser-beam self-focusing), and have attributed it to the four-wave-mixing process described above. A spectrum of the transmitted laser beam is shown in Fig. 4(a) under conditions of a laser power density of $\sim 1\times 10^8$ W/cm^2, a laser detuning of 2.4 Å to the short-wavelength side of the D_2 resonance line, a sodium number density of 1×10^{14} cm^{-3}, and an argon buffer gas of 1 Torr pressure. Figure 5 establishes that the emitted radiation is in fact at

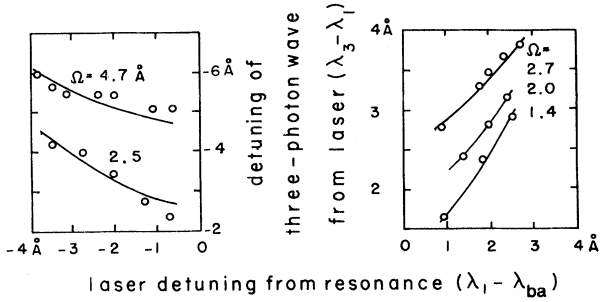

FIG. 5. Wavelength difference between one sideband (the one whose detuning from resonance has the same sign as that of the incident laser) and the laser is plotted against the laser detuning from resonance for several values of the laser intensity given in terms of the Rabi frequency in wavelength units. Solid curves give the value of the generalized Rabi frequency of Eq. (1).

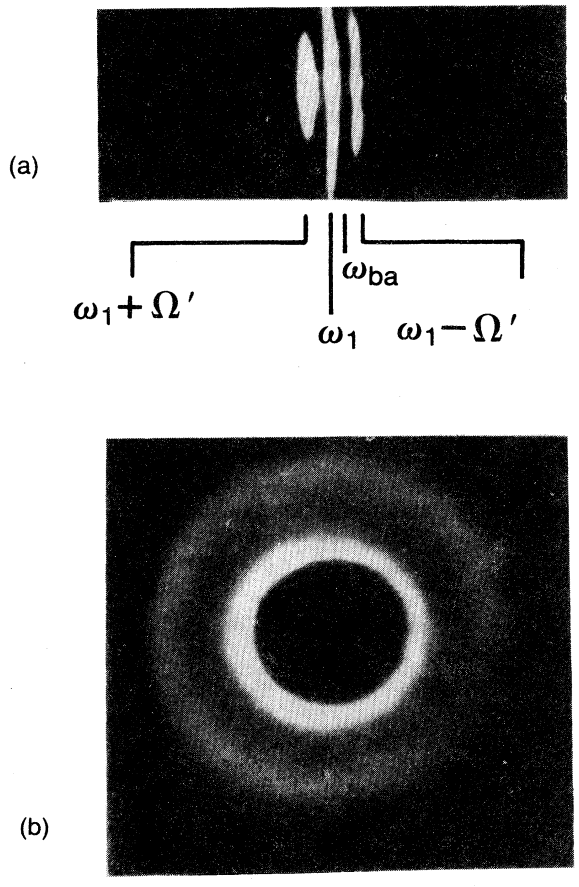

FIG. 4. (a) Spectrum of the light leaving the sodium cell in the forward direction. The central feature is at the frequency of the incident laser, while the sidebands are symmetrically displaced by the generalized Rabi frequency. The incident laser was focused to the power density of $\sim 1\times 10^8$ W/cm^2 into a vapor of sodium atoms $\sim 1\times 10^{14}$ cm^{-3} with a detuning of 2.4 Å to the short-wavelength side of the D_2 line. (b) At sodium densities $\geq 1\times 10^{15}$ cm^{-3}, the laser beam experiences self-focusing, leading to the emission of the lower-frequency sideband in a cone surrounding the transmitted laser beam. The central portion of the laser beam is blocked to avoid saturating the film.

the Rabi frequency by comparing the measured value of the wavelength shift to the theoretical value determined by the value of the Rabi frequency. It was also reported in Ref. 12 that at higher sodium densities ($\sim 10^{15}$ cm^{-3}) and input intensities corresponding to $\Omega/\Delta=0.1$, self-trapping occurred leading to a strong spectral broadening of the sidebands and to the emission of the lower-frequency sideband in a cone surrounding the transmitted laser as shown in Fig. 4(b). We have since determined that the spectral peak of this conical emission occurs at a frequency shifted from that of the laser by an amount that is in the range from 1.5 to 3.0 Δ, with the particular value depending on experimental conditions. This result is consistent with the range of values appearing in the data of Meyer,[18] and also is consistent with the observation of Skinner and Kleiber[15] that the frequency shift is always about 2.0Δ. We propose that this conical-emission phenomenon (which has also been observed by many others[14,15,18–20]) is due to four-wave mixing enhanced by the ac Stark effect in self-trapped filaments. We present here a series of observations in support of this model. According to this model, the observed spectral shift (1.5—3.0 Δ) of the conical emission must be equal to the generalized Rabi frequency Ω' given by Eq. (1), and hence, the ratio Ω/Δ within a self-trapped filament must fall in the range 1.1—2.8. We have measured the laser intensity within individual self-trapped filaments (as discussed in Sec. IV) and have found that under all experimental conditions in which conical emission is produced, the ratio Ω/Δ does fall within this narrow range. Theoretical considerations of the formation of self-trapped filaments are developed in Sec. III and show that this result is to be expected. In addition, in order for the Rabi sideband generation process to be efficient, there must be significant gain for Ω/Δ in this range. Figure 3 shows the theoretical value of the gain plotted as a function of Ω/Δ for typical values of the experimental parameters and shows that there is significant gain for the value of Ω/Δ of interest. Furthermore, in order for the laser intensity to be nearly constant spatially and temporally, it is necessary that a stable self-trapped filament be formed. We present theoretical and

experimental evidence in Secs. III and IV, respectively, that such is, in fact, the case. The spectral broadening of the conical emission can result from several effects, one of which is the intensity variations which shift the resonance frequencies of the four-wave-mixing process via the Rabi frequency and self-phase modulation.

The angle of the conical emission produced by four-wave mixing in a self-trapped filament is determined by phase matching and by refraction at the filament boundary.[21] The refractive index inside the filament can be assumed to be unity due to saturation, while the index of the surrounding region is that of the unsaturated atomic vapor as shown in Fig. 6. Thus, for a positive laser detuning, the three-photon wave (on the high-frequency side of resonance) will be trapped inside the filament while the fourth parametric wave (on the low-frequency side of resonance) is refracted out of the filament at an angle θ which according to Snell's law is given by

$$\theta=[\theta_0^2+2\,\delta n(\omega_4)]^{1/2}\,, \tag{2}$$

where θ_0 is the internal angle and $\delta n(\omega_4)$ is the change in refractive index across the filament boundary for the frequency of the conical emission.

Figure 7 shows the measured half-angle of the conical emission plotted (a) as a function of laser detuning at a fixed number density of 1.6×10^{15} cm^{-3} and (b) as a function of atomic number density at a fixed detuning of 2 Å. The curves are given by an empirical formula that relates the conical-emission angle to the unsaturated refractive index $1+\delta n(\omega_1)$ of the pump laser as

$$\theta=k\,|\,2\,\delta n(\omega_1)\,|^{1/2}\,, \tag{3}$$

with $k=1.8$. The data presented in Fig. 3 of Skinner and Kleiber[15] is well fitted by Eq. (3) with $k=2.0$. Brechignac *et al.*[20] also presents data which fit this equation but without sufficient information to find a value of k. The phenomenological model presented by Skinner and Kleiber,[15] and based on a hypothetical nonresonant four-wave-mixing process, results in a value $k=\sqrt{2}$, while the transient theory of LeBerre-Rousseau *et al.*[22] predicts $k=1.0$.

In previous discussions of the conical-emission angle it had been assumed that $\delta n(\omega_4)$ was equal to $-\delta n(\omega_1)$, since it was believed that the peak frequency of the cone spectrum and the laser frequency were symmetrically displaced from the atomic resonance frequency. However, it

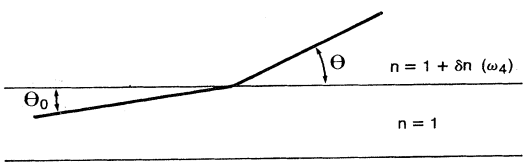

FIG. 6. Conical-emission results from the refraction of the low-frequency sideband at the boundary of the self-trapped filament, while the high-frequency sideband remains trapped by total internal reflection. The observed angle θ is related by Eq. (2) to the internal angle θ_0 which depends on phase-matching considerations.

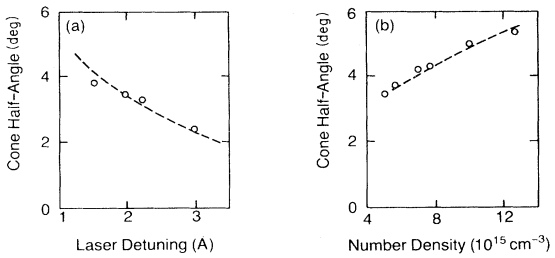

FIG. 7. Conical-emission angle plotted (a) as a function of laser detuning and (b) as a function of atomic number density. Curves are an empirical relation given by Eq. (3).

is not correct to make this assumption since it has been reported by Meyer[18] and confirmed by ourselves that the spectral peak of the cone is not always 2Δ from the laser frequency. Also, the spectral width of the conical emission is much too great to ignore the dispersion in $\delta n(\omega_4)$. In order to relate the empirically determined Eq. (3) to the theoretical Eq. (2) it would be necessary to determine the functional form of θ_0. Since the internal angle θ_0 is determined by phase matching, it depends upon the dispersion characteristics of light within self-trapped filaments, which is poorly understood at present. In addition, there is experimental evidence (see Sec. IV) that at least one of the pump waves is a "leaky" mode of the self-trapped filament, which further complicates the determination of θ_0.

III. SELF-FOCUSING AND SELF-TRAPPING

The four-wave-mixing process leading to Rabi sideband generation is profoundly modified by self-focusing of the laser beam, both because the value of the Rabi frequency is increased as a result of self-focusing and because the phase-matching considerations that determine the angular distribution of the emitted radiation are modified by the intensity-dependent change in the refractive index that accompanies self-focusing. In fact, conical emission of the generated radiation was observed only in the presence of self-focusing. In this section we briefly review the theory of self-focusing and self-trapping and then treat in more detail two aspects of self-focusing that play a key role in the interpretation of our experimental results: (1) the temporal evolution of the nonlinear atomic response and (2) the resulting intensity distribution within a self-trapped filament. We shall use the term self-focusing to mean any intensity-dependent focusing of the laser beam and the more restrictive term self-trapping to mean the propagation of a self-focused beam with a diameter that is nearly constant in space and time.

Self-focusing and self-trapping of a laser beam tuned to the high-frequency side of an atomic resonance was first predicted by Javan and Kelley.[23] Their treatment predicts that a light beam initially of diameter d will be brought to a focus in a distance of the order of

$$z_f=d\,[n_0/16\,\delta n(\omega_1)]^{1/2}\,, \tag{4}$$

where n_0 is the unsaturated refractive index of the medium at the laser frequency ω_p and $\delta n(\omega_1)$ is the light-

induced change in the refractive index. Their analysis also predicts the possibility of self-trapping of the light beam resulting from the tendency of the beam to diverge due to diffraction being exactly balanced by the focusing effect of the nonlinear refractive index. If the diffraction half-angle ($\sim 1.22\lambda/2n_0 d$) is equal to the critical angle for total internal reflection [$\sim(2\delta n/n_0)^{1/2}$], then the diameter d of the filament corresponds to the minimum possible diameter for self-trapping which is given by

$$d_{\min}=1.22\lambda[8n_0\,\delta n(\omega_1)]^{-1/2}\,. \tag{5}$$

Here λ is the vacuum wavelength of the incident radiation. In an atomic vapor an intense laser beam can totally saturate the refractive index, in which case $\delta n(\omega_1)=n_0(\omega_1)-1$. Filament diameters close to the minimum diameter given by Eq. (5) have been observed by Grishkowsky[17] in potassium vapor.

We have found experimentally (see Sec. IV) that the intensity within a self-trapped filament is always such that Ω/Δ is in the range 1.1—2.8. The origin of this small range of unique values is saturation of the refractive index. As long as the refractive index continues to increase with increasing field strength, the nonlinear medium acts as a lens with positive power, leading to continued focusing and a further increase in the optical intensity. This self-focusing process must terminate when the refractive index saturates, which occurs roughly when $\Omega\sim\Delta$. A somewhat more detailed prediction of the field strength within a self-trapped filament can be obtained by modeling the filament as a step-index waveguide as discussed later in this section.

Chiao *et al.*[24] have shown the existence of a solution to the nonlinear wave equation corresponding to a self-trapped filament of light for the case of a medium with a $\chi^{(3)}$ nonlinearity. This solution corresponds to a single central spot and for a given value of $\chi^{(3)}$ it corresponds to a given radial intensity distribution and hence to a fixed value of the power. Haus[25] later showed the existence of higher-order solutions to be same equation corresponding to a central spot surrounded by a number of rings. Each such solution also has a fixed radial intensity distribution. Marburger *et al.*[26] have found similar results in their computer simulation of self-focusing in a medium with a saturating nonlinear refraction index that follows the field intensity with no time delay.

A. Temporal evolution of the atomic response

Most of the experiments reported in this paper and in Refs. 14, 15, 18, 19, and 20 were conducted under conditions such that

$$\Delta^{-1}<T_2<\tau_p<T_1\,, \tag{6}$$

where τ_p denotes the laser-pulse length and where T_1 and T_2 denote the longitudinal and transverse relaxation times, respectively. Under these conditions, the medium does not necessarily come to steady state during the laser pulse, and hence it is not obvious that steady-state self-trapping should be possible under these conditions. However, as the laser intensity increases due to self-focusing, rapid Rabi oscillations tend to equilibrate the level populations in a time of the order Ω^{-1}, which can be much shorter than τ_p. A theoretical demonstration of this fact is presented in the next paragraph; supporting experimental evidence is presented in Sec. IV.

Under conditions (6), the refractive index experienced by a pump wave at frequency ω_1 is given by

$$n(\omega_1)=1+2\pi N\,\mathrm{Re}[\mu_{ab}\rho_{ba}(\omega_1)/E_1]\,, \tag{7}$$

where the notation is the same as in previous work,[11] namely, N denotes the atomic number density and $\rho_{ba}(\omega_1)$ denotes the component of the off-diagonal element of the density matrix oscillating at frequency ω_1. The temporal evolution of $\rho_{ba}(\omega_1)$ can be found by solving the density-matrix equation of motion [Eq. (3) of Ref. 11] in the rate-equation limit. The rate-equation approximation is valid so long as

$$\left|\frac{\delta(\rho_{bb}-\rho_{aa})}{\delta t}\right|\ll 1/T_2\,. \tag{8}$$

For $\Delta\gg 1/T_2$, this condition is met whenever $\Omega\ll\Delta$. For a pulse with a sudden turn on at time $t=0$, the refractive index at a time $t\gg T_2$ (that is, after any coherent transients have died out) is given by

$$n=1-\frac{2\pi|\mu_{ab}|^2}{\hbar(\Delta^2+1/T_2^2)}\left[(\rho_{bb}-\rho_{aa})^0\exp\left[-\left[\frac{1}{T_1}+\frac{1}{T_2}\frac{\Omega^2}{\Delta^2+1/T_2^2}\right]t\right]\right.$$
$$\left.+(\rho_{bb}-\rho_{aa})^{\mathrm{dc}}\left\{1-\exp\left[-\left[\frac{1}{T_1}+\frac{1}{T_2}\frac{\Omega^2}{\Delta^2+1/T_2^2}\right]t\right]\right\}\right], \tag{9}$$

where $(\rho_{bb}-\rho_{aa})^0$ is the initial population difference and $(\rho_{bb}-\rho_{aa})^{\mathrm{dc}}$ is the dc component of the steady-state population difference given by

$$(\rho_{bb}-\rho_{aa})^{\mathrm{dc}}=(1+\Delta^2T_2^2)(\rho_{bb}-\rho_{aa})^0/(1+\Delta^2T_2^2+\Omega^2T_1T_2)\,. \tag{10}$$

The refractive index thus reaches its steady-state value in a time of the order of T_1 for weak fields, but for strong fields it reaches steady state in a time of the order of $T_2(\Delta/\Omega)^2$. This behavior for strong fields is due to dephasing of the Rabi oscillations.

Under typical experimental conditions with $T_2/T_1\sim 0.02$ and $T_2/\tau_p\sim 0.06$, the Rabi frequency before the occurrence of self-focusing is less than $\sim 0.5\Delta$

and the value of the Rabi frequency within a self-trapped filament is such that $\Omega/\Delta \sim 2$. In the case that $\Omega/\Delta > 1$, condition (7) is not met due to Rabi oscillations. Thus an analysis of the refractive index based entirely on the rate-equation approximation is not necessarily valid. However, it can be seen from Eq. (9) that for $T_2 \ll T_1$ the population difference $(\rho_{bb} - \rho_{aa})$ will be nearly saturated even before Ω increases to a value comparable to Δ. Thus, near the center of the self-trapped filament, the refractive index will be nearly equal to unity as predicted by the steady-state theory. However, near the boundary of the filament, where $\Omega \ll \Delta$, the atomic response will be in the transient regime. Self-focusing under these conditions cannot be described in either the pure steady-state or pure transient limits discussed by Shen and co-workers.[27] However, many of the aspects of self-trapping, such as filament diameters, depend only upon the total change in refractive index between the center of the filament and the surrounding medium, which can therefore be calculated under the assumption of steady-state conditions. In addition, the fact that the atomic response quickly reaches its steady state near the center of the filament indicates that the steady-state model of four-wave mixing presented in Ref. 11 is applicable for these experiments which use pulsed lasers.

B. Optical waveguide model of self-trapped filaments

Many of the properties of a self-trapped filament of light can be obtained by treating the filament as a step-index optical waveguide as shown in Fig. 8. The refractive index of the central region is assumed to be equal to unity while that of the surrounding region is equal to that of the unsaturated atomic vapor n_0. This model ignores the complication (as discussed above) imposed by the small boundary region in which the refractive index is only partially saturated. The theory of step index, weakly guided ($|n_0 - 1| \ll 1$) waveguides has been developed for use in fiber optics and is applied here. Gloge[28] has shown that an axially symmetric electric-field distribution linearly polarized in the y direction of a guided wave in such a structure, is given by

$$E_y = E_0 J_0(ur/a)/J_0(u) , \quad r < a \tag{11a}$$

$$E_y = E_0 K_0(wr/a)K_0(w) , \quad r \geq a \tag{11b}$$

where $J_0(\xi)$ and $K_0(\xi)$ denote the lowest-order Bessel and modified Hankel functions, respectively, r is the radial coordinate, a is the radius of the central region, and E_0 is the electric-field strength at the waveguide boundary. The parameters u and w are defined in terms of the propagation constant β of the guided wave as

$$u \equiv a(k^2 - \beta^2)^{1/2} , \tag{12a}$$

$$w \equiv a(\beta^2 - k^2 n_0^2)^{1/2} , \tag{12b}$$

where $k = \omega/c$. Only axially symmetric field distributions are considered here because of the symmetry of the self-focusing process. These solutions are known as linearly polarized $LP_{0,m}$ modes, where $m - 1$ is an integer denoting the number of zeros of $J_0(ur/a)$ lying in the range $0 < r < a$, and thus the number of rings surrounding the bright central spot. These solutions are further restricted by a boundary condition of the form[28]

$$uJ_{-1}(u)/J_0(u) = -wK_{-1}(w)/K_0(w) . \tag{13}$$

For the case of self-trapped filaments in which the optical radiation forms and then is guided by the waveguide, an additional restraint is imposed by the requirement that the central lobe of the electric-field distribution must have a diameter (full width at half maximum intensity) no smaller than $d_{\min}$ of Eq. (5). It is shown in Sec. IV that the (FWHM) diameter d of the central lobe of the self-trapped filaments is always approximately equal to $d_{\min}$. The requirement that $d = d_{\min}$, along with the constraint given by Eq. (13), is sufficient to determine u, w, and a, and thus to determine the electric-field distribution uniquely by Eqs. (11) in terms of its value E_0 at the boundary of the waveguide. This field distribution is shown in Fig. 8. Numerically, it is found that for the lowest-order mode $m = 1$ (which is most commonly observed in these experimental studies), the peak value of the electric field at $r = 0$ is 2.5 times larger than E_0. For a self-trapped filament, E_0 is the minimum electric-field amplitude that is sufficient to saturate the refractive index. As was discussed in connection with Eq. (8), saturation will occur under those experimental conditions when the field strength is such that the ratio Ω/Δ is in the range 0.5—1.0. Thus it is expected that the peak value of the Rabi frequency in a self-trapped filament will be such that the ratio Ω/Δ lies in the range 1.25—2.5—in good qualitative agreement with the measured values as will be discussed in Sec. IV.

IV. EXPERIMENTAL RESULTS

The apparatus used in the experimental work reported here is illustrated in Fig. 9. A frequency-doubled Nd:YAG laser pumps a Littman-style dye laser[10] that pro-

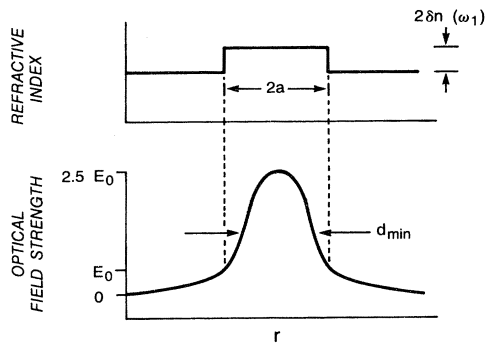

FIG. 8. A self-trapped filament is modeled as a step-index optical waveguide of diameter $2a$ and refractive-index difference $\delta n(\omega_1)$. If it is assumed that the (FWHM) filament diameter is equal to $d_{\min}$ of Eq. (5) as required by self-focusing theory, the electric-field distribution of Eqs. (11) has the illustrated form. The maximum value of the electric field is thus ~ 2.5 times the value at the boundary of the filament.

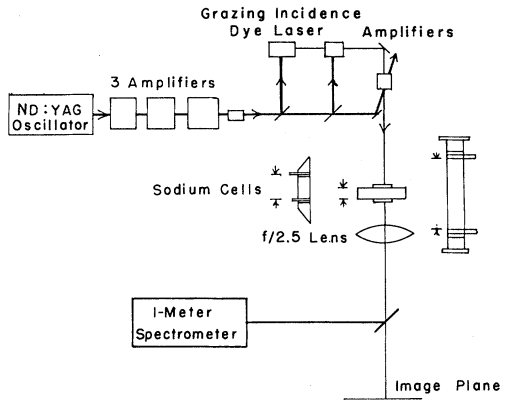

FIG. 9. Experimental setup. A single-mode Nd:YAG laser pumps a single-mode rhodamine-6G dye laser. The spatially filtered output of the dye laser is focused into one to three sodium vapor cells, the output of which is collected by a well-corrected $f/2.5$ lens. The output is studied spectroscopically, photographically, and radiometrically, as described in the text.

duces 2—7 nsec pulses. Each of these lasers runs in a single longitudinal mode to prevent intensity modulation due to mode beating that can wash out the Rabi sideband structure of the atomic response. Typical peak powers measured at the laser are 1.0 MW. The laser is tuned to the high-frequency side of the $(3^2S_{1/2}$-$3^2P_{3/2})D_2$ line of sodium at 5890 Å. The laser beam is spatially filtered and is focused into one of several sodium vapor cells. Heat pipe ovens with vapor region lengths of 2.5 and 25 cm and a cell with hot sapphire windows with a 1.25-cm path length were used.

Since conical emission is produced in self-trapped filaments, experiments were done to characterize their properties. In order to observe self-trapped filaments, a well-corrected $f/2.5$ lens was used to form a magnified image of the exiting laser beam. Figure 10(a) shows the beam exiting the empty 2.5 cm cell. This structureless beam was formed by removing the rings of an Airy diffraction pattern using an aperture. In the remainder of the photographs shown in Fig. 10, the sodium number density was $\sim 5\times 10^{15}$ cm^{-3}, the laser detuning was 2 Å, and self-trapped filaments leading to conical emission were present. Figure 10(b) shows the beam self-focused into a single filament. To obtain this photograph the input laser power was adjusted to the minimum value (~ 40 kW/cm^2) that produced self-focusing. As the laser power is increased, the exiting beam breaks up into more than one filament as shown in Fig. 10(c). It was found that the power in each filament is approximately (to within a factor of 3) the same, and that the effect of increasing the laser power is to increase the number of filaments but not the power in each filament. This observation is in agreement with the predictions of Bespalov and Talanov.[29] When the incoming laser beam has nearly uniform intensity, as it does in Fig. 10(c), it is found that the locations of filaments change randomly from shot to shot. However, if structure is purposely introduced on the incident laser beam (for instance by placing a diffracting aperture immediately before the cell), the positions of the filaments stay fixed from shot to shot as is shown in Fig. 10(e). The ability to produce filaments in fixed locations has allowed the measurement of the intensity and temporal behavior of the light leaving a single filament, as will be discussed later. Figure 10(d) shows the beam exiting the 1.25 cm cell. The incoming laser intersects the sapphire windows of this cell at nearly normal incidence leading to an interference pattern that also tends to fix the locations of the individual filaments.

In order to demonstrate that stable self-trapping has occurred, we have compared the measured diameter of our laser beam at the exit window of the 1.25 cm cell to the theoretical value of $d_{\min}$ for a self-trapped filament. This comparison is shown in Fig. 11, where the theoretical value is obtained from Eq. (5) with $\delta n(\omega_1)$ determined from the measured cone angle using the experimentally determined relation, Eq. (3). In addition, the temporal behavior of the light emerging from a single self-trapped filament was measured by imaging the filament onto a silicon pin photodiode along with a delayed portion of the input beam. The diameter of the active area of the detector was smaller than the product of $Md_{\min}$ where M is the magnification of the optical system. Therefore, this measurement compares the temporal behavior of the intensity within the self-trapped filament with that of the incident laser. A trace of the detector output as produced by a Tektronix 519 oscilloscope is shown in the inset to Fig. 11.

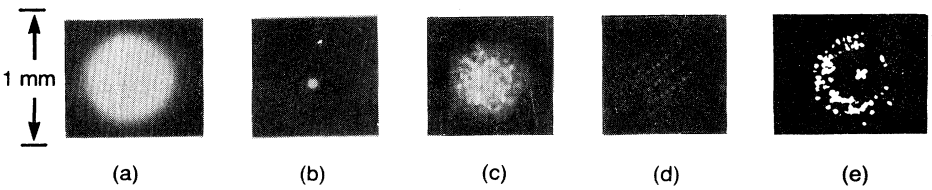

FIG. 10. Images of the laser beam at the exit window of the sodium cell. (a) Exiting beam in the absence of self-focusing, obtained by detuning the laser from resonance. (b) The beam has self-focused into a single filament. (c) At higher incident power the beam breaks up into many filaments. The positions of these filaments can be fixed by introducing structure on the incident-beam profile, by (d) interference fringes produced by a sapphire window, or (e) Fresnel diffraction.

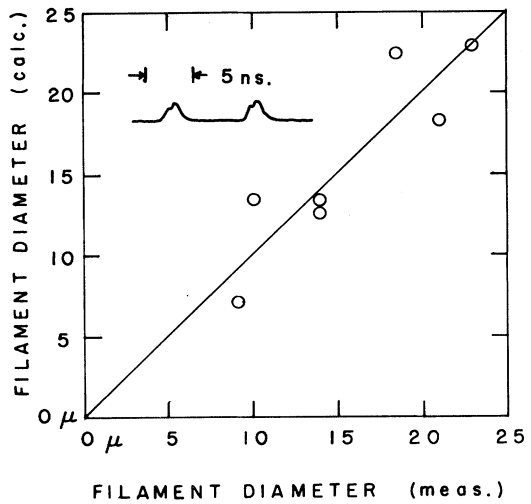

FIG. 11. Measured filament diameters (FWHM) are compared with theoretical values given by the measured cone angle using Eq. (3). The inset shows an oscilloscope trace comparing the temporal behavior of the light leaving the filament with a delayed portion of the input laser beam.

The intensity of the transmitted light follows closely that of the incident radiation. In addition, no radiation was detected when the detector was moved transversely by a distance greater than $d_{\min}M$. These observations show that trapping has occurred and that the filament diameter does not change appreciably during the laser pulse.

In order to determine the value of the Rabi frequency within individual self-trapped filaments a calibrated detector was used to measure the power contained within filaments of known diameter. The measured intensity is used to calculate the Rabi frequency which is expressed as a wavelength shift in Å. These results are plotted in Fig. 12 as a function of the laser detuning from resonance. The two dotted lines in this graph delineate the range of Ω/Δ (1.1—2.8) inferred from the observed spectral shift of the conical emission under the assumption that this shift is equal to the Rabi frequency. The vertical lines terminated with crosses give the range of intensities that were observed within self-trapped filaments using the 2.5 cm cell at a fixed laser detuning when the atomic number density, the laser power, focusing characteristics of the input beam, and the pressure of the buffer gas were all varied. The only restriction that was imposed in determining this range was that the conical emission be present and that distinct filaments be observed. In calculating the Rabi frequency we assumed that the beam diameter was equal to $d_{\min}$ as given by Eq. (5) because for this cell we were unable to measure the beam diameter directly due to refraction at the nonabrupt sodium—buffer-gas boundary. Also shown in Fig. 12 are data obtained using the 1.25 cm cell where we were able to measure the beam diameter directly at the abrupt sodium-sapphire boundary. In this case no buffer gas was present and only the sodium density was varied to obtain the indicated range. The observed intensities (i.e., Rabi frequencies) span a surprisingly small range at a given value of the laser detuning, presenting strong evidence that self-focusing is limited by processes of the sort mentioned in Sec. III. In addition, the observed Rabi frequencies are in the correct range to account for conical emission as a Rabi sideband phenomenon.

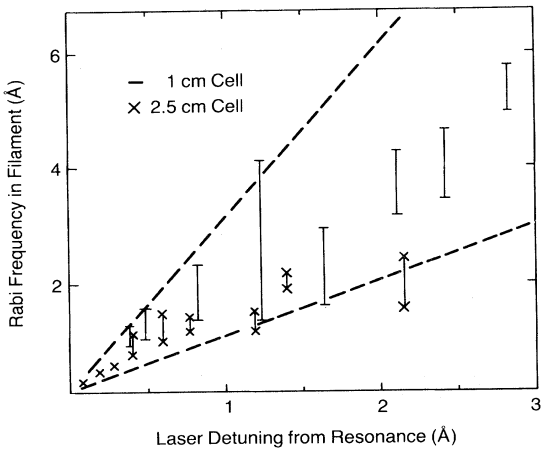

FIG. 12. Observed range of intensities within self-trapped filaments (expressed as a Rabi frequency in Å units) is shown as a function of the laser detuning from resonance. This range coincides with that inferred from the observed spectrum of the conical emission which is indicated by the two dashed lines.

Another experiment showed that the change in refractive index responsible for self-trapping was the result of the transfer of the ground-state population to the sodium excited state. In this experiment a second tunable laser was used to form a probe beam that crossed the path of the pump laser in the sodium vapor. It was found that when self-trapping of the pump laser occurred, the probe laser was scattered from the self-trapped filament forming a partial cone as shown in Fig. 13(a). The occurrence of this phenomenon was found to be relatively insensitive to the angle between the two beams and to the wavelength of the probe beam so long as it was nearly resonant with one of the sodium D lines. Only when the wavelengths of the two lasers were nearly the same, the angle between the beams was properly adjusted, and the pump power was reduced to avoid self-focusing, was multiple beam scattering of the sort reported by Heer[30] observed. We also observed strong scattering of the probe beam off the self-trapped filament when the probe beam was delayed by as much as 12 nsec with respect to the pump laser beam. A delay of 24 nsec was sufficient to inhibit any observable scattering. These observations suggest that steady-state self-trapping has occurred and that the self-trapped filament can in fact be modeled as a dielectric waveguide that decays away with the 16 nsec lifetime of the sodium $3p$ level. Tam and Happer[31] have reported bouncing one beam of light off another beam in sodium vapor. Their experiment was performed using a cw laser, and their observation is attributed to optical pumping of the sodium ground state. Optical pumping should not play an important role in our experiment because our laser pulse duration is much less than the radiative lifetime of the sodium excited state.

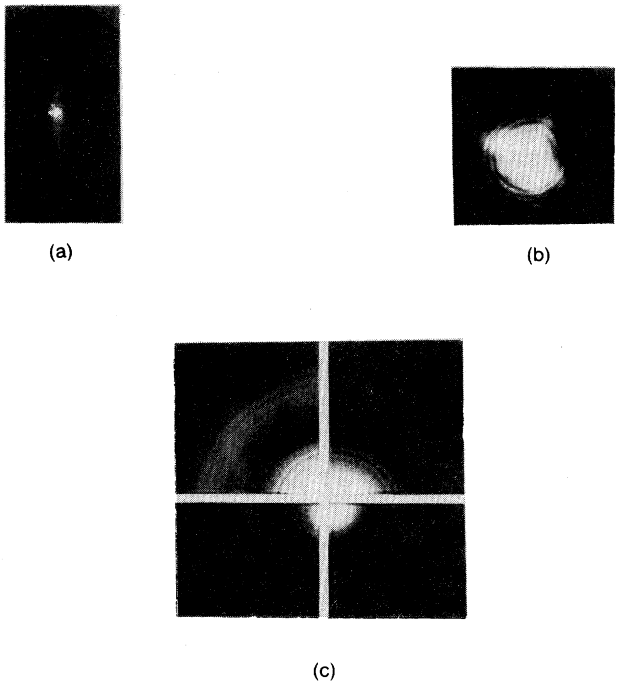

FIG. 13. (a) Far-field diffraction patterns of the probe beam as scattered off a self-trapped filament. Such scattering is observed only when the time delay between the pump and probe beams is less than 24 nsec. (b) Magnified image of the laser beam exiting the cell when the beam has self-focused into a high-order self-trapped filament. (c) Far-field diffraction pattern of a high-order self-trapped filament similar to that shown in (b).

Our observation that the filament decays in a time comparable to the radiative lifetime of the excited state provides additional support for this interpretation.

Conical emission. The efficiency of converting the self-focused light into the conical emission was measured in the 25 cm cell for a laser detuning of 3.7 Å. The energy in the cone was found to be 1×10^{-8} J and the energy in the single, self-focused filament (of 25 μm diameter) was found to be 2×10^{-7} J giving a conversion efficiency of 5%. The overall conversion efficiency, that is, the ratio of the power in the conical emission to the input laser power was found to be several times lower and dependent on the input beam parameters which determine the efficiency of the self-focusing process.

The minimum filament diameter $d_{\min}$ predicted by Eq. (5) scales as $[\delta n(\omega_1)]^{1/2}$, where $\delta n(\omega_1)$ depends on the atomic number density N and laser detuning Δ as N/Δ^2. It was found that by varying N and Δ it was possible to observe structureless filaments whose diameters ranged from 5 to 50 μm. The lower limit was imposed by absorption of the pump laser as it was tuned close to the atomic resonance to increase δn. There appears to be no fundamental upper limit on filament diameter, although self-focusing distances become excessively long when δn is decreased. For similar reasons it was possible to observe self-focusing and hence conical emission for laser detunings in the range 0.04—10 Å, and for sodium densities in the range 2.5×10^{14}—1.2×10^{16} cm^{-3}. Conical emission was always observed for diameters less than 25 μm. For larger diameters conical emission was observed in the 25 cm cell, but not in either of the shorter cells. It is believed that this is because the gain of the four-wave-mixing process as modified by the presence of the filament is smaller for the larger diameter filaments. To test this idea an opaque object was placed next to the laser beam near the center of the 25 cm sodium cell. For a filament of small diameter (14 μm) this object cast a strong (dark) shadow in the conical emission indicating that most of the emission was occurring in the first half of the cell. From the cone angle measured far from the cell and the measured diameter of the cone at the exit window it was estimated that conical emission was occurring only from the first 2 to 3 cm of the cell. When a filament larger than 25 μm was formed only a weak shadow was cast on the conical emission showing that conical emission was taking place over the entire length of the cell. In this case the cone was filled in at the exit window but was not filled in far from the cell, indicating conical emission from the entire cell. It was also found that if the exiting filament was focused onto the entrance slit of a monochromator the low-frequency sideband was present only in the case where the conical emission was still being generated at the end of the cell. For the small diameter (14 μm) filament only light at the laser frequency was present in the filament at the end of the cell and no radiation was observed emitted from the filament for the last 22 to 23 cm of the cell. A possible explanation for this dependence on the filament diameter is that at least one of the pump waves is a leaky mode of the self-trapped filament. The propagation distance of a leaky mode can be estimated by applying the loss equation (Eqs. 1.5—13 from Ref. 32) for a leaky mode of a slab waveguide. It is found that for the waveguide of about 15 μm thickness the leaky mode propagates approximately 0.5 cm, and with a thickness of 50 μm it propagates approximately 5 cm—in agreement with the observed conical-emission generation length. The observation that the 14 μm filament propagates for $\sim$22 cm without generating Rabi sidebands seems to indicate that guided pump modes do not generate Rabi sidebands. A possible explanation is that perfect phase matching prohibits this process.

We have also observed self-trapped filaments having a higher-order mode structure, as has been predicted by Haus.[25] If an exceptionally clean beam is focused into the sodium cell, a large fraction of the light focuses into a single filament consisting of a central core surrounded by concentric rings. The formation of filaments with similar structure has also been explained by Marburger *et al.*[26] as resulting from spherical aberration of the self-focusing process. As the laser beam self-focuses, the intensity-dependent change in refractive index eventually saturates, leading to lower focusing in the center of the beam than near its edges. A photograph of such a filament as it leaves the sodium region is shown in Fig. 13(b). This fig-

ure bears a striking resemblance to the photographs of a spherically aberrated focus as illustrated in the text of Born and Wolf.[33] The far-field diffraction pattern of this filament and the conical emission are shown in Fig. 13. Note the high correlation between the structure of the transmitted laser light at the larger angles and of the parametrically generated conical emission surrounding the central spot.

V. DISCUSSION

It has been shown that an intense, near resonant laser field can, through the ac Stark effect, modify the energy-level structure of an atomic system in such a way as to create a new resonance in the nonlinear susceptibility describing nearly degenerate four-wave mixing. This resonance leads to a strong coupling between two weak waves symmetrically detuned from the intense field by the generalized Rabi frequency. In the absence of such coupling, radiation at one Rabi sideband would in general be amplified by the stimulated three-photon effect, while radiation at the other sideband would experience the ac-Stark-shifted absorption of the atomic transition. However, we have shown theoretically and verified experimentally that, when the interaction is properly phase matched, the strong coupling due to the ac-Stark-shift-induced resonance can lead to the simultaneous growth of radiation at both sidebands.

We have also observed experimentally that at sufficiently large sodium densities the pump laser self-focuses within the vapor cell. The self-trapped filaments thus formed are remarkably stable in that their diameters are nearly constant during the duration of the exciting pulse and in that the filaments persist for more than 10 nsec after the exciting pulse exits the vapor cell. The intensity of the light contained within each such filament is found to depend on the laser detuning from resonance Δ in such a way that the Rabi frequency Ω is between 1 and 3 times Δ. In the presence of self-focusing, four-wave mixing still occurs but the lower-frequency sideband is emitted in the form of a cone surrounding the transmitted laser beam. The conical-emission angle is within a factor of 2 of that predicted by Snell's law under the assumption that the sideband is generated in the forward direction as measured inside the filament. The spectral peak of the conical emission is shifted from that of the exciting laser by a value in the range from 1 to 3 Δ, in agreement with the measured value of the Rabi frequency.

ACKNOWLEDGMENTS

The authors gratefully acknowledge discussion of these effects with D. G. Hall, P. Narum, M. G. Raymer, and C. R. Stroud, Jr. This work was supported by the U. S. Army Research Office.

---

*Present address: Allied Corporation, 7 Powderhorn Drive, Mt. Bethel, NJ 07060.

[1]A. M. Bonch-Bruevich and V. A. Khodovoi, Usp. Fiz. Nauk. 93, 71 (1967) [Sov. Phys. Usp. 10, 637 (1968)]; P. L. Knight and P. W. Milonni, Phys. Rep. 66, 21 (1980).

[2]C. Cohen-Tannoudji and S. Reynaud, J. Phys. B 10, 345 (1977); E. Courtens and A. Szoke, Phys. Rev. A 15, 1588 (1977); 17, 2119(E) (1978).

[3]S. H. Autler and C. H. Townes, Phys. Rev. 100, 703 (1955).

[4]B. R. Mollow, Phys. Rev. 188, 1969 (1969).

[5]F. Schuda, C. R. Stroud, Jr., and M. Hercher, J. Phys. B 7, 1198 (1974).

[6]F. Y. Wu, S. Ezekial, M. Ducloy, and B. R. Mollow, Phys. Rev. Lett. 38, 1077 (1977).

[7]N. Bloembergen and Y. R. Shen, Phys. Rev. 133, A37 (1964).

[8]B. R. Mollow, Phys. Rev. A 7, 1319 (1973).

[9]T. Fu and M. Sargent III, Opt. Lett. 4, 366 (1979).

[10]D. J. Harter and R. W. Boyd, IEEE J. Quantum Electron. QE-16, 1126 (1980).

[11]R. W. Boyd, M. G. Raymer, P. Narum, and D. J. Harter, Phys. Rev. A 24, 411 (1981).

[12]D. J. Harter, P. Narum, M. G. Raymer, and R. W. Boyd, Phys. Rev. Lett. 46, 1192 (1981).

[13]P. D. Kleiber, K. Burnett, and J. Cooper, Phys. Rev. A 25, 1188 (1982).

[14]G. L. Burdge and C. H. Lee, Appl. Phys. B 28, 197 (1982).

[15]C. H. Skinner and P. D. Kleiber, Phys. Rev. A 21, 151 (1979).

[16]A. C. Tam, Phys. Rev. A 19, 1971 (1978).

[17]V. M. Arutyunyan, N. N. Badalyan, V. A. Iradyan, and M. E. Mousesyan, Zh. Eksp. Teor. Fiz. 60, 66 (1971) [Sov. Phys.—JETP 33, 34 (1971)].

[18]Y. H. Meyer, Opt. Commun. 34, 434 (1980).

[19]D. Grischkowsky, Phys. Rev. Lett. 24, 866 (1970).

[20]G. Brechignac, Ph. Cahuzac, and A. Debarre, Opt. Commun. 35, 87 (1980).

[21]C. A. Sacchi, C. H. Townes, and J. R. Lifsitz, Phys. Rev. 174, 439 (1968).

[22]M. LeBerre-Rousseau, E. Ressayre, and A. Tallet, Opt. Commun. 36, 31 (1980).

[23]A. Javan and P. L. Kelley, IEEE J. Quantum Electron. QE-2, 470 (1966).

[24]R. Y. Chiao, E. Garmire, and C. H. Townes, Phys. Rev. Lett. 13, 479 (1964).

[25]H. A. Haus, Appl. Phys. Lett. 8, 128 (1966).

[26]J. H. Marburger and E. Dawes, Phys. Rev. Lett. 21, 556 (1968); E. L. Dawes and J. H. Marburger, Phys. Rev. 179, 862 (1968).

[27]Y. R. Shen and M. T. Loy, Phys. Rev. A 3, 2099 (1970); E. G. Hanson and Y. R. Shen, Opt. Commun. 20, 45 (1977).

[28]D. Gloge, Appl. Opt. 10, 2252 (1971).

[29]V. I. Bespalov and V. I. Talanov, Zh. Eksp. Teor. Fiz. Pis'ma Red. 3, 425 (1966) [JETP Lett. 3, 307 (1966)].

[30]C. V. Heer and N. C. Griffen, Opt. Lett. 4, 239 (1979).

[31]A. C. Tam and W. Happer, Phys. Rev. Lett. 38, 278 (1977).

[32]D. Marcuse, *Theory of Dielectric Waveguides* (Academic, London, 1974), pp. 1—94.

[33]M. Born and E. Wolf, *Principles of Optics* (Pergamon, Oxford, 1975), p. 479.

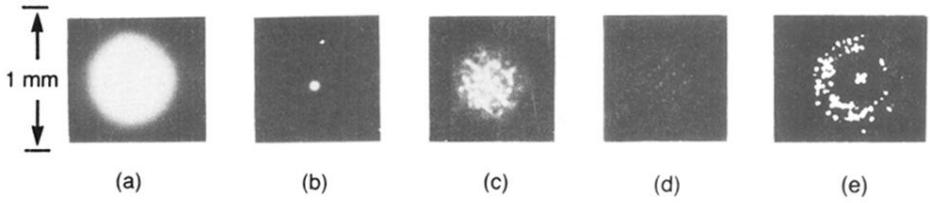

FIG. 10. Images of the laser beam at the exit window of the sodium cell. (a) Exiting beam in the absence of self-focusing, obtained by detuning the laser from resonance. (b) The beam has self-focused into a single filament. (c) At higher incident power the beam breaks up into many filaments. The positions of these filaments can be fixed by introducing structure on the incident-beam profile, by (d) interference fringes produced by a sapphire window, or (e) Fresnel diffraction.

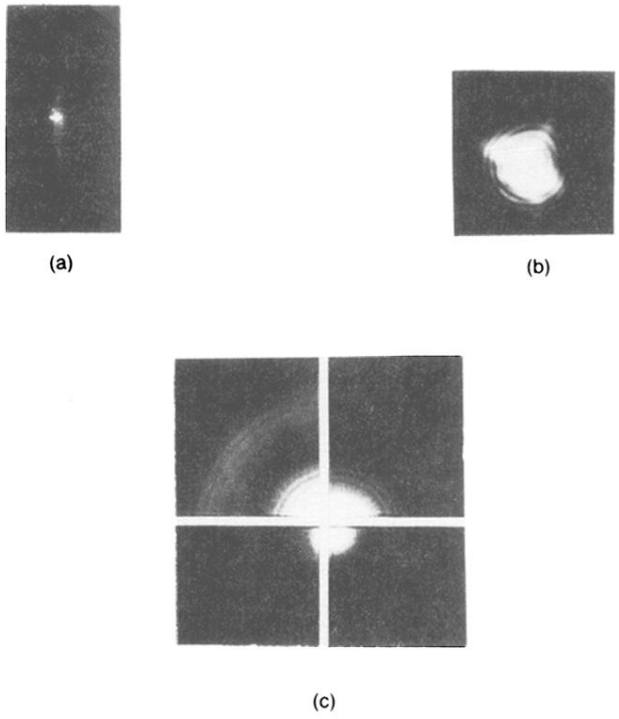

FIG. 13. (a) Far-field diffraction patterns of the probe beam as scattered off a self-trapped filament. Such scattering is observed only when the time delay between the pump and probe beams is less than 24 nsec. (b) Magnified image of the laser beam exiting the cell when the beam has self-focused into a high-order self-trapped filament. (c) Far-field diffraction pattern of a high-order self-trapped filament similar to that shown in (b).

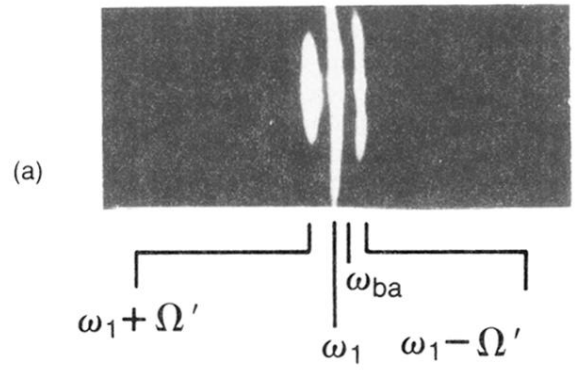

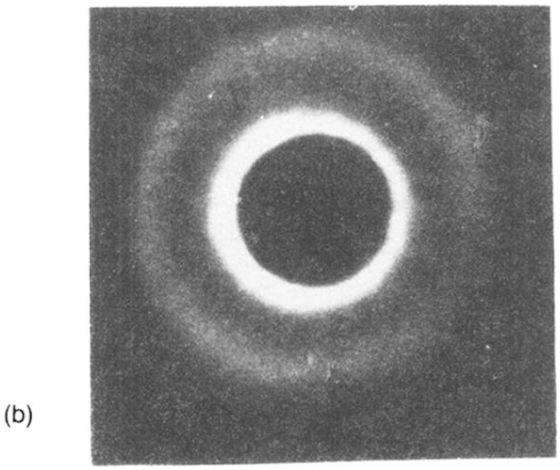

FIG. 4. (a) Spectrum of the light leaving the sodium cell in the forward direction. The central feature is at the frequency of the incident laser, while the sidebands are symmetrically displaced by the generalized Rabi frequency. The incident laser was focused to the power density of $\sim 1\times 10^{8}$ W/cm^2 into a vapor of sodium atoms $\sim 1\times 10^{14}$ cm^{-3} with a detuning of 2.4 Å to the short-wavelength side of the D_2 line. (b) At sodium densities $\geq 1\times 10^{15}$ cm^{-3}, the laser beam experiences self-focusing, leading to the emission of the lower-frequency sideband in a cone surrounding the transmitted laser beam. The central portion of the laser beam is blocked to avoid saturating the film.